Thermodynamic properties of selected glasses in the CaO–Al2O3–TiO2 system

Anatoly Arkhipin, Alexander Pisch, Georgii Zhomin, Semen Kuzovchikov, Alexandra Khvan, Natalia Smirnova, Alexey Markin, Nikita Kovalenko, Irina Uspenskaya

Thermodynamic properties of selected glasses in the $CaO-Al_2O_3-TiO_2$ system

Anatoly S. Arkhipin [a,b,c,*], Alexander Pisch [c], Georgii M. Zhomin [b], Semen V. Kuzovchikov [d], Alexandra V. Khvan [d], Natalia N. Smirnova [e], Alexey V. Markin [e], Nikita A. Kovalenko [a], Irina A. Uspenskaya [a]

[a] Department of Chemistry, Lomonosov Moscow State University, 119991, Leninskie Gory, 1/3, Moscow, Russia

[b] Department of Materials Science, Lomonosov Moscow State University, 119991, Leninskie Gory, 1/73, Moscow, Russia

[c] University Grenoble Alpes, CNRS, Grenoble INP, SIMaP, F-38000, Grenoble, France

[d] Thermochemistry of Materials SRC, NUST MISIS, 119049, Moscow, Russia

[e] Department of Chemistry, National Research Lobachevsky State University of Nizhny Novgorod, 603950, Nizhny Novgorod, Russia

KEYWORDS: calcium aluminate, calcium aluminotitanate, C12A7, heat capacity, heat content, enthalpy of formation.

* Corresponding Author: E-mail address: Arkhipin@td.chem.msu.ru (A.S. Arkhipin)

ABSTRACT

The thermodynamic properties of a $Ca_{12}Al_{14}O_{33}$ (C12A7) binary glass and the impact of titania additives (+5 and 7wt.%) were studied for the first time using three different calorimetric techniques: low-temperature adiabatic, high-temperature drop solution and transposed temperature drop calorimetry. The enthalpy of formation from oxides at 298.15 K of $Ca_{12}Al_{14}O_{33}$ and $Ca_{12}Al_{14}O_{33}$+7wt.% TiO_2 glass samples (16.0±1.8 and 14.8±2.4 kJ/mol, respectively) and the enthalpy of dissolution of TiO_2 at 1073.15 K were obtained by drop solution calorimetry in a $2PbO\text{-}B_2O_3$ solvent. A close value (11.9±2.3 kJ/mol) was obtained for the same C12A7 glass by transposed temperature drop calorimetry. The investigation of the impact of TiO_2 additions on the thermodynamic properties of glasses shows that there is no influence on heat capacity of C12A7 up to 7wt.% of TiO_2. In contrast, a negative deviation of the enthalpy of formation from oxides at 298.15 K from the ideal-mixing straight line was observed.

(Alex, remember, that 150 words is a maximum in the Abstract)

1. Introduction

The importance of high-quality thermodynamic data for glasses is growing in many fields: geo-chemistry and earth science, industrial glass production and novel low CO_2 building materials. For example, to lower the specific CO_2 content of a cement, one of the key strategies is to replace the high CO_2 component (crystalline clinker) by various low CO_2 cementitious materials (slags, fly ashes, natural pozzolanas, calcined clays). Many of them are largely amorphous in nature. To predict their reactivity using thermodynamic and kinetic modeling, the enthalpy of formation and Gibbs energy in the range from 0 °C / 273.15 K to 100 °C / 373.15 K must be known. The feasibility of this approach was illustrated by the recent works by Kucharczyk et al [1] and Zajac et al [2].

Thermodynamic properties of amorphous materials can be obtained either by theoretical calculations (molecular dynamics – classical or ab-initio) or by experimental work using different calorimetric techniques. Both methods are time consuming, so the reasonable combination of experimental and calculating approaches will allow us to get the most useful information while reducing the time required to conduct research. In order to get high-quality theoretical data, ab-initio molecular dynamics is the method of choice using supercells of maximum size. This was shown recently for CaO [3] and in the CaO-Al_2O_3-TiO_2 ternary system [4]. However, the validity of these data always needs to be verified, so experimental data on the thermodynamic properties of the systems under study are necessary. In terms of experimental methods, the low-temperature heat capacity is obtained using low-temperature adiabatic calorimetry [5,6] or relaxation calorimetry [7,8]. For temperatures above room temperature, differential scanning calorimetry for glasses [6,9] and high-temperature drop calorimetry for both glasses and liquids [10,11] can be used. The enthalpy of formation of oxide glasses is usually determined by drop solution calorimetry in various solvents (lead borate, sodium molybdate) [12–14]. It should be noted that the thermodynamic properties of glasses are generally less well studied than those of crystalline substances. Therefore, new data on the values of thermodynamic functions of glasses obtained using a complex of methods and complementing each other will provide additional arguments in the discussion of whether glasses should be considered frozen (unstable) or metastable states. And a comparison of the properties of crystalline and amorphous samples of identical composition can be useful for quantitative characterization of amorphization processes.

Something about CAT system and potential application of obtained experimental data Following the CALPHAD approach, low-dimensional systems should be studied at the beginning. Glasses in the binary CaO-Al_2O_3 system are well known from a structural point of view [15–19]. From compositions between 50 ($CaAl_2O_4$, CA) > Al_2O_3 > 25 ($Ca_3Al_2O_6$, C3A) mol.%, aluminum is only in tetrahedral coordination in glasses and the number of bridging oxygens vary between 4 to 2 respectively for CA and C3A [18,19]. Calcium evolves from a regular 6-fold coordination for C3A glass up to 7-fold for CA glass composition [17]. No work is known on ternary glasses with TiO_2.

Except structural properties of glasses in the CaO-Al_2O_3 binary system, the phase diagram information about the melting points for both binary CaO-Al_2O_3 [20] and ternary CaO-

Al_2O_3-TiO_2 [21] systems were reported. In addition, Richet et al [8] conducted an experimental investigation of the low-temperature heat capacity of a binary C3A glass sample and estimated the heat capacity of glasses in the whole CaO-Al_2O_3-SiO_2 system using the additive contribution approach. Besides, Navrotsky et al [14] carried out drop solution experiments in the $x$$Ca_{0.5}AlO_2$–(1-$x$)$SiO_2$ glass section in lead borate solvent at 985 K.

The purpose of this work is to investigate the thermodynamic properties of a $Ca_{12}Al_{14}O_{33}$ (C12A7) binary glass and the influence of titania additives on these properties. Two $Ca_{12}Al_{14}O_{33}$ + $x$$TiO_2$ ternary glasses were prepared and investigated to achieve the second goal. Three different calorimetric techniques: low-temperature adiabatic, high-temperature drop solution and transposed temperature drop calorimetry was used. Obtained data may be useful for modeling the use of amorphous material in building materials and for CALPHAD use in high temperature slags for Ti rich steel alloys.

It was claimed by Navrotsky [13] that a lead borate solvent is not suitable for drop solution calorimetry for samples with TiO_2, due to precipitation formation. However, in a newer publication [29] the authors concluded that a lead borate solvent could be used for titania, but with limitation of the number of drops. However, for TiO_2 we found only one paper with drop solution calorimetry using a lead borate solvent [29]. In this article the authors conducted drop solution experiments at 973 and 1046 K. For the calculation of the enthalpy of formation from the oxides of studied glass, it is required to have data at 1073.15 K. Thus, additional task was devoted to conducting the drop solution experiments of TiO_2 (rutile) at 1073.15 K in 2PbO-B_2O_3 molten solvent.

Thus, the absence of thermodynamic properties of glasses in the ternary CaO-Al_2O_3-TiO_2 system and the presence of only estimated heat capacity data for a C12A7 glass sample makes this investigation actual and important.

2. Experimental Section

2.1.Starting Materials

The manufacturers, CAS Registry Numbers (CASRN) and purities of chemical samples used in this work are listed in Table 1. All chemicals were used without further purification.

Table 1. Sources and Purities of Chemicals.

chemical name	CASRN	source	purity
$CaCO_3$, calcium carbonate	471-34-1	Alfar Aesar	> 99.95%[a]
α-Al_2O_3, aluminium oxide	1344-28-1	Alfar Aesar	> 99.9%
TiO_2, titanium dioxide, rutile	1317-80-2	Alfar Aesar	> 99.8%[a]

[a] Metal base

2.2. Glass synthesis

The synthesis of glasses was carried out by the classical method of quenching in water. The starting materials $CaCO_3$, α-Al_2O_3 and TiO_2 (rut) were dried in air for 12 hours in a muffle furnace at 300 °C / 573.15 K, 1000 °C / 1273.15 K and 300 °C / 573.15 K, respectively. The initial powders were mixed in a calculated amount in a mixer. The resulting mixture was then calcined in a Pt/Au crucible at 1000 °C / 1273.15 K for 1 hour to remove CO_2. After that, the temperature in the furnace was raised to 1600 °C / 1873.15 K (100–200 K above the liquidus temperature of the mixture) and the sample was kept for 2 hours. The samples were quenched by soaking the bottom of the crucible in water for ~ 10 seconds. The resulting glass was ground in an automatic agate mortar. Then the powder was again melted at 1600 °C / 1873.15 K. The procedure was repeated 3 times to obtain homogenized samples. To confirm the absence of crystalline phases, powder X-ray diffraction (powder XRD) and Raman-spectrometry measurements were conducted. No crystalline phases in the studied samples were detected, which indicates that the resulting samples are amorphous (see Figure S1).

Glasses in the binary CaO-Al_2O_3 ($12CaO\text{-}7Al_2O_3$ = C12A7 in reduced oxide notation), and ternary CaO-Al_2O_3-TiO_2 ($12CaO\text{-}7Al_2O_3$ + 5 wt.% TiO_2 and + 7 wt.% TiO_2) systems were selected for our study. The C12A7 glass sample is an amorphous analogue of the mineral mayenite $Ca_{12}Al_{14}O_{33}$, the labeling of samples with titanium correspond to different amounts of TiO_2 added to sample C12A7 (+5 wt.% TiO_2 and + 7 wt.% TiO_2).

The chemical composition and molar masses of the studied glass samples are summed up in Table 2.

Table 2. Composition of studied glasses.

Name	Formula / 1 atom	ω, %			*M*, g/mol
		CaO	Al_2O_3	TiO_2	
C12A7	$(CaO)_{0.632}(Al_2O_3)_{0.368}$	48.5	51.5	0	72.982
C12A7+5T	$(CaO)_{0.603}(Al_2O_3)_{0.351}(TiO_2)_{0.046}$	46.1	48.9	5	73.297
C12A7+7T	$(CaO)_{0.591}(Al_2O_3)_{0.345}(TiO_2)_{0.064}$	45.1	47.9	7	73.425

2.3.Low-temperature adiabatic calorimetry

2.3.1. Experimental procedure

A BCT precision automatic adiabatic calorimeter (Termis, Moscow) was used to measure the isobaric heat capacities ($C_{p,m}$) of calcium aluminate and calcium titanoaluminate glasses over the temperature range of (10–350) K. The principal, design and operation of the calorimeter were described in detail earlier [22]. All measurements were performed with a computer-controlled measuring system comprising of an analog-to-digital converter, a digital-to-analog converter, and a switch.

The calorimetric cell is a thin-walled cylindrical vessel made from titanium with a volume of 1.5 cm^3. It was loaded with a sample and then degassed in vacuum with a residual pressure of ≈ 5 Pa. Dry helium gas ($x(H_2O) < 2 \cdot 10^{-4}$ %) at p = 4 kPa and room temperature was introduced into the cell to facilitate heat transfer during the measurements. An iron-rhodium resistance thermometer (nominal resistance 100 Ω; calibrated on ITS-90 standard by the Russian Metrology Research Institute, Moscow, Russia) placed on the inner surface of the adiabatic shield was used for the temperature measurements. The difference in temperature between the ampule and an adiabatic shield was controlled by a four-junction copper-iron-chromel thermocouple; the sensitivity of the thermometric circuit was 10^{-3} K. After assembling,

the measuring system was cooled in a liquid nitrogen bath. If the measurements were performed below 80 K, a liquid helium bath was used. The ampule with the substance was filled with dry helium as a heat exchange gas to the pressure of 4 kPa at room temperature. Heat capacity measurements were continuously and automatically carried out by means of the standard method of intermittently heating the sample and alternately measuring the temperature. The cooling of the samples to the temperature of the measurement onset was performed at a rate of 10^{-2} K/s. Then the samples were heated with a temperature step of (0.5–2) K at a rate of 10^{-2} K/s. The sample temperature was recorded after an equilibration period (temperature drift < 10^{-2} K/s, approximately 10 min per experimental point). The ratio of the sample heat capacity to the total (sample + cell) one was between 0.4 to 0.7. Each sample was first measured in the liquid nitrogen region, followed by measurements from liquid helium with overlapping temperature intervals of the two series.

The relative standard uncertainty in heat capacity measurements $C_{p,m}$ was estimated as 0.2%·over the main temperature range of (40–350) K, 0.5%·between T = (20–40) K, and within 2% at T < 20 K. These values were verified using standard reference samples (benzoic acid and α-Al_2O_3).

2.3.2. Heat capacity measurements approximation

One of the accurate and effective methods for the approximation of the experimental heat capacity as a function of temperature is the semi-empirical Planck-Einstein approach [23]. It allows to approximate the experimental heat capacity and heat content data and to extrapolate the $C_p(T)$ data in the wide temperature range. In this approach the heat capacity is described by Equation 1:

$$C_p(T) = 3R\sum_{i=1}^{N} \alpha_i \frac{\left(\frac{\Theta_i}{T}\right)^2 e^{\frac{\Theta_i}{T}}}{\left(e^{\frac{\Theta_i}{T}}-1\right)^2} \quad (1)$$

where α_i, Θ_i (i = 1, 2, …) – are adjustable parameters that are selected in such a way as to best describe the adiabatic calorimetry data.

The derived thermodynamic functions are obtained by integration of the corresponding expressions (Equations 2–3), using the optimized parameters in the Equation 1:

$$H^o(T) - H^o(0) = \int_0^T C_p(T)dT = 3R\sum_{i=1}^{N} \alpha_i \frac{\frac{\Theta_i}{T}}{e^{\frac{\Theta_i}{T}}-1} \quad (2)$$

$$S^o(T) - S^o(0) = \int_0^T \frac{C_p(T)}{T} dT = 3R\sum_{i=1}^{N} \alpha_i \left(\frac{\frac{\Theta_i}{T}}{e^{\frac{\Theta_i}{T}}-1} - \ln\left(1 - e^{-\frac{\Theta_i}{T}}\right)\right) \quad (3)$$

All modeling steps were conducted using the CpFit software [24]. The α_i and Θ_i parameters are found by the least squared method using the next object function χ^2:

$$\chi^2 = \sum_{i=1}^{N} \omega_i \left[\frac{C_{p,i}^{calc}(T_i) - C_{p,i}^{exp}(T_i)}{C_{p,i}^{exp}(T_i)}\right]^2 \quad (4)$$

where $C_{p,i}^{calc}(T_i)$ – heat capacity calculated from Equation 1 at T_i; $C_{p,i}^{exp}(T_i)$ – experimental heat capacity at T_i; ω_i – defined statistical weights (default values are $\omega_i = 1/\delta_{exp}$, where δ_{exp} – relative deviation of the experimental values (see paragraph above)).

2.4.High temperature drop calorimetry

2.4.1. Experimental procedure of the enthalpy of dissolution measurements

High temperature drop solution calorimetry was used for the experimental determination of the enthalpy of formation from oxides of glasses with respect to the constituent oxides in their crystalline reference state. The commercial isoperibol Tian-Calvet calorimeter Alexsys 1000 (Setaram, France) was used for drop dissolution experiments. The detailed information about the experimental procedure is described in the paper [25]. This instrument is equipped with a 3D Calvet sensor, which provides high sensitivity and exceptional precision. The measurement system comprises two Inconel tubes that reach into the hot zone of the furnace. Quartz glass tubes that contain the molten solvent and gas-flushing and bubbling systems are inserted into inconel tubes. Both sides of the calorimeter were used during one set of experiments.

Before each series of experiments, the calibration of the calorimeter was performed. For that, 7–11 reproducible drops of 4–17 mg high purity alumina (99.95% from NIST) were dropped in empty platinum crucibles that were in calorimeter. The calibration factors were determined with uncertainties less than 1%. Heat increments between room temperature and the temperature inside the calorimeter (800 °C / 1073.15 K) were calculated from the Standard Reference Material equation [26].

Well characterized glass samples (pellets 3–13 mg) were dropped into a lead borate melt (n(PbO) / n(B_2O_3) = 2.008; 20.00(30.00)±0.05 g) which was used as a solvent and was located in platinum crucibles. This solvent was chosen because of the rapid dissolution of CaO and Al_2O_3 in it. The temperature inside the calorimeter was 800 °C (1073.15 K). All experiments were carried out under atmospheric pressure (the rate of artificial air flow was 10 mL/min). Additionally, dry air (x(H_2O) < $5 \cdot 10^{-4}$ %) was bubbled through the solvent with rate 5 mL/min to aid in dissolution by providing constant mixing and to ensure a high oxygen fugacity in the melt in order to maintain a consistent oxidation state of the dissolved oxides. Dissolution of each sample in the molten solvent was complete within about 1.5 h. The lead borate solvent was changed for «fresh» one after each series of experiment. The software Calisto from Setaram was used for recording the output signals and processing the heat flux curves from the calorimeter.

2.4.2. Experimental procedure of the enthalpy of crystallization measurements

The heat effect of crystallization of the binary C12A7 glass was measured by transposed temperature drop calorimetry using a SETARAM MHTC96 drop calorimeter (type S measuring head). Two different temperatures were chosen, 998 °C / 1271.15 K and 1098 °C / 1371.15 K. The calorimeter was calibrated at each temperature using pure, sintered Al_2O_3 pieces (99.95% Alfa Aesar) with a mass ranging from 20 to 80 mg each. The measured surface area of the integrated heat flux was plotted against the theoretical heat content. Again, the NIST reference data was used for the theoretical heat content data for alumina. The calibration constant was obtained by linear regression of the measured data points with fixed origin at zero. The observed uncertainty corresponds to two times the standard deviation of the slope and lies between 1% and 1.2% depending on the temperature of the measurement. The enthalpy of crystallization was obtained by dropping up to 6 pieces of glass into the calorimeter for a single run. The enthalpy value was obtained by plotting the measured integral heat flux versus the introduced mass. The reported uncertainty corresponds to the joint uncertainty of the measurement and the calibration constant using twice the standard deviation of the slope. In order to obtain the enthalpy of crystallization at room temperature, the recrystallized samples were dropped a second time to measure their heat content to the temperature of the calorimeter.

3. Results

3.1.Low-temperature adiabatic calorimetry

The low-temperature heat capacity $C_p(T)$ of C12A7, C12A7+5T and C12A7+7T samples were measured by adiabatic calorimetry. The results are presented in Figure 1. The curves were shifted to 10 and 20 J/(mol·K) for C12A7+5T and C12A7+7T respectively to avoid the "sticking" curves. The raw data are listed in Tables S1–S3 in Supplementary Information.

After analyzing the data obtained for the glass samples in the nitrogen region, it was found that the $C_p(T)$ values for all samples coincide within the measurement error bars. Thus, the C12A7+7T sample was only measured in the nitrogen temperature range (90–350 K) (green circles in Figure 1) to optimize the time and material costs of research. In order to recreate the correct behavior of the heat capacity function to 0 K for C12A7+7T glass, some points were calculated in the helium region (10–90 K) by the linear combination of C_p values for C12A7 and C12A7+5T samples (these points are filled green squares in Figure 1). A very low-temperature region (10–30 K) is presented in the insertion in Figure 1. The dashed lines are the extrapolation of heat capacity to 0 K.

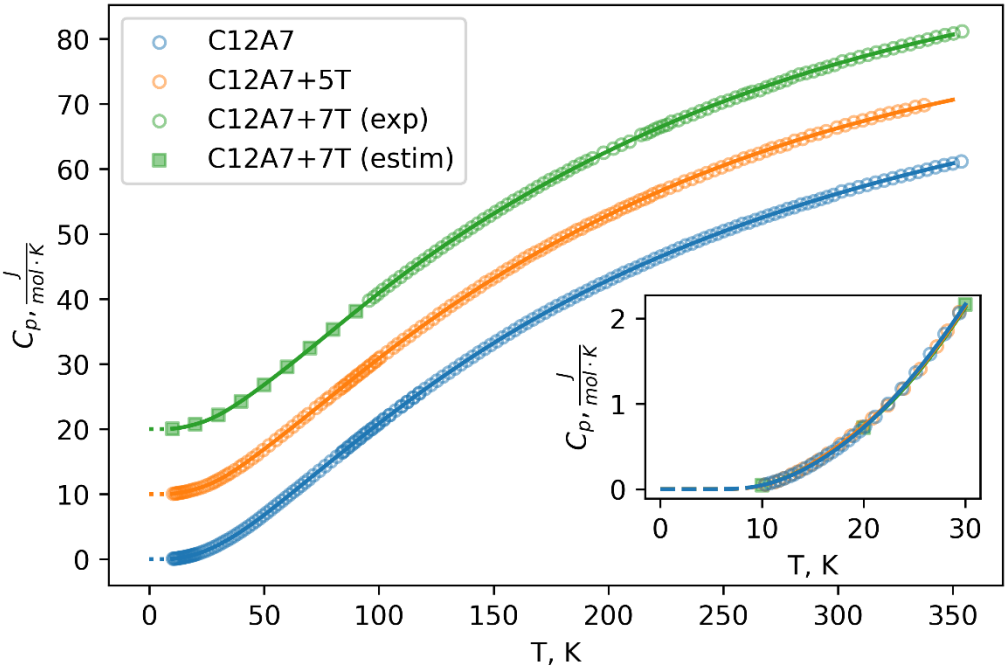

Figure 1. Heat capacities (J/(mol·K)) of C12A7, C12A7+5T, C12A7+7T; the curves are shifted to 10 and 20 J/(mol·K) for C12A7+5T and C12A7+7T, respectively. The empty circles–

experimental data (see Tables S1–S3), the filled squares – estimated data for C12A7+7T by linear combination of C12A7 and C12A7+5T samples data (see Table S3), solid lines – Planck-Einstein approximation (see Equation 1 and Table 3), dashed lines – Planck-Einstein extrapolation to 0 K (see Equation 1 and Table 3). Insertion: a very low-temperature region (0–30 K) for all of samples without shifts. Data are normalized to 1 mole of formula unit of glass.

A numerical analysis of the semiempirical Planck-Einstein model [23] was performed for each dataset (using Equation 1 and Table 3) and the obtained curves were added to Figure 1. The fitting parameters α_i, Θ_i determined by minimization of object function χ^2 (see Equation 4) are presented in Table 3. Values are given with an excess number of significant digits to reproduce the calculation results of this study.

Table 3. Parameters of Planck-Einstein model for C12A7, C12A7+5T and C12A7+7T glass samples (see Equations 1–4).

Parameter	C12A7	C12A7+5T	C12A7+7T
α_1	1.2444±0.045	1.2334±0.059	1.2686±0.036
θ_1, K	651.7±27.2	457.1±14.2	440.1±12.5
α_2	0.7793±0.045	1.1495±0.050	1.2063±0.038
θ_2, K	1381.7±116.2	973.6±45.8	993.6±31.1
α_3	0.8803+0.038	0.6565±0.024	0.6071±0.023
θ_3, K	322.1±9.6	204.9±2.8	197.8±3.7
α_4	0.3712±0.021	0.0954±0.002	0.0858±0.003
θ_4, K	169.5±2.8	82.3±0.5	80.0±0.6
α_5	0.0723±0.0016	-	-
θ_5, K	77.7±0.4	-	-

The thermodynamic functions (C_p, $S^o(T)$–$S^o(0)$, $H^o(T)$–$H^o(0)$) were calculated using the parameters from Table 3 and Equations 1–3 and are presented in Tables 4–6.

Table 4. Smoothed thermodynamic properties of C12A7 glass.

T, K	C_p, $\frac{\text{J}}{\text{mol}\cdot\text{K}}$	$H^o(T)-H^o(0)$, $\frac{\text{kJ}}{\text{mol}}$	$S^o(T)-S^o(0)$, $\frac{\text{J}}{\text{mol}\cdot\text{K}}$

10	0.0462	0.000059	0.00669
20	0.7226	0.00327	0.2029
30	2.163	0.01706	0.7425
40	4.256	0.04871	1.638
50	6.790	0.1037	2.854
100	20.87	0.7963	11.89
150	33.23	2.159	22.78
200	42.91	4.074	33.72
250	50.38	6.414	44.14
298.15	56.04±0.11	8.981±0.018	53.51±0.18
300	56.23	9.085	53.86
350	60.86	12.02	62.89
400[a]	64.55	15.16	71.27
450[a]	67.49	18.46	79.04
500[a]	69.85	21.89	86.28

[a] Extrapolated data

Table 5. Smoothed thermodynamic properties of C12A7+5T glass.

T, K	C_p, $\frac{\text{J}}{\text{mol}\cdot\text{K}}$	$H^\circ(T)-H^\circ(0)$, $\frac{\text{kJ}}{\text{mol}}$	$S^\circ(T)-S^\circ(0)$, $\frac{\text{J}}{\text{mol}\cdot\text{K}}$
10	0.0430	0.000052	0.00586
20	0.7411	0.00337	0.2083
30	2.145	0.0171	0.7462
40	4.326	0.0490	1.647
50	6.903	0.1049	2.885
100	20.88	0.7982	11.94
150	33.16	2.161	22.82
200	42.93	4.072	33.75
250	50.53	6.417	44.18

298.15	56.12±0.11	8.991±0.018	53.58±0.20
300	56.30	9.095	53.93
350[a]	60.64	12.02	62.95
400[a]	63.91	15.14	71.27
450[a]	66.41	18.40	78.95
500[a]	68.33	21.77	86.05

[a] Extrapolated data

Table 6. Smoothed thermodynamic properties of C12A7+7T glass.

T, K	C_p, $\frac{\text{J}}{\text{mol} \cdot \text{K}}$	$H^\circ(T) - H^\circ(0)$, $\frac{\text{kJ}}{\text{mol}}$	$S^\circ(T) - S^\circ(0)$, $\frac{\text{J}}{\text{mol} \cdot \text{K}}$
10	0.0460	0.000058	0.00647
20	0.726	0.00335	0.2077
30	2.128	0.0169	0.7382
40	4.286	0.0485	1.632
50	6.819	0.1038	2.857
100	20.92	0.7949	11.87
150	33.14	2.159	22.76
200	42.78	4.066	33.67
250	50.37	6.403	44.07
298.15	56.03±0.11	8.970±0.020	53.45±0.45
300	56.22	9.074	53.79
350	60.66	12.00	62.81
400[a]	64.04	15.12	71.14
450[a]	66.63	18.39	78.84
500[a]	68.63	21.78	85.97

[a] Extrapolated data

The differences between experimental heat capacity (Tables S1–S3) and calculated by Equation 1 and parameters from Table 3 for all studied sample are shown in Figure 2. As we can see, the deviations for almost all points are less than 0.4% for T > 50 K, and 2% from 10 to 50 K. Keep in mind that the uncertainty 0.2% of heat capacity values above 50 K is estimated with respect to C_p of reference substances without considering the possible scatter of real samples measurements, we believe that the parameters of the Planck-Einstein equation adequately describe the experimental data.

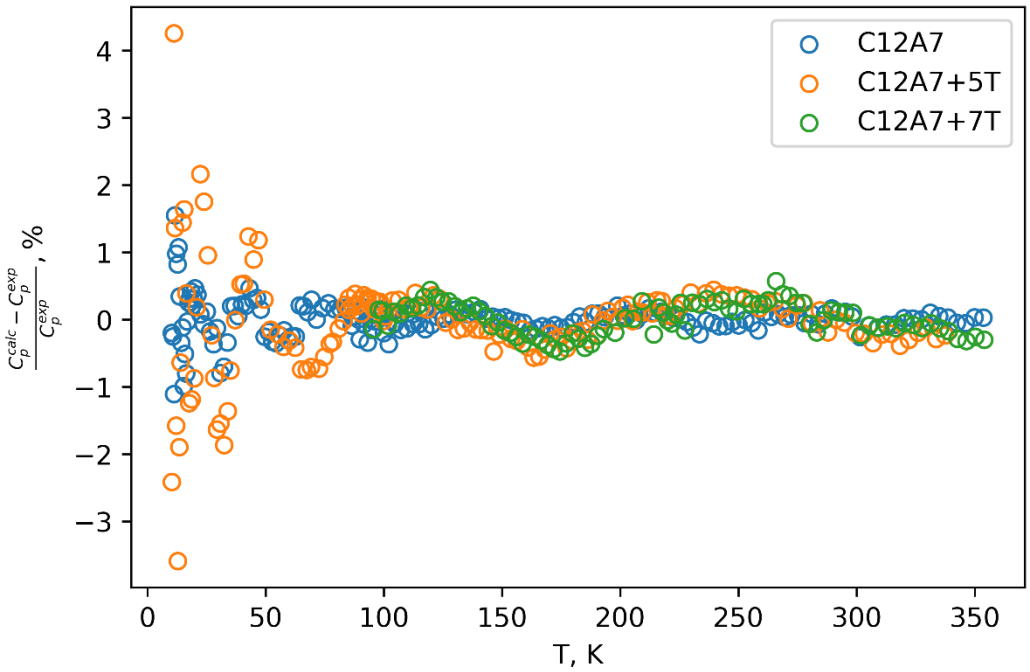

Figure 2. Differences between experimental heat capacity (Tables S1–S3) and calculated by Equation 1 and parameters from Table 3 for all the studied samples.

3.2. High-temperature drop solution calorimetry

All raw data of drop solution experiments (mass of sample, mass of solvent, number of drops, room temperature, calorimeter temperature, solvent number, enthalpy of drop solution for each drop) of C12A7 and C12A7+7T glass samples are summarized and listed in Table S4 in the Supplementary Information. To be sure that during the whole series, experiments were carried out in the infinitely dilute solution, the dependences of the enthalpy of dissolution of

C12A7 and C12A7+7T glass samples as mole fraction of the dissolved sample in the lead borate solvent were calculated and plotted in Figure 3a. No composition dependence of the thermal effect on the total amount of the studied sample in the lead borate solvent was revealed.

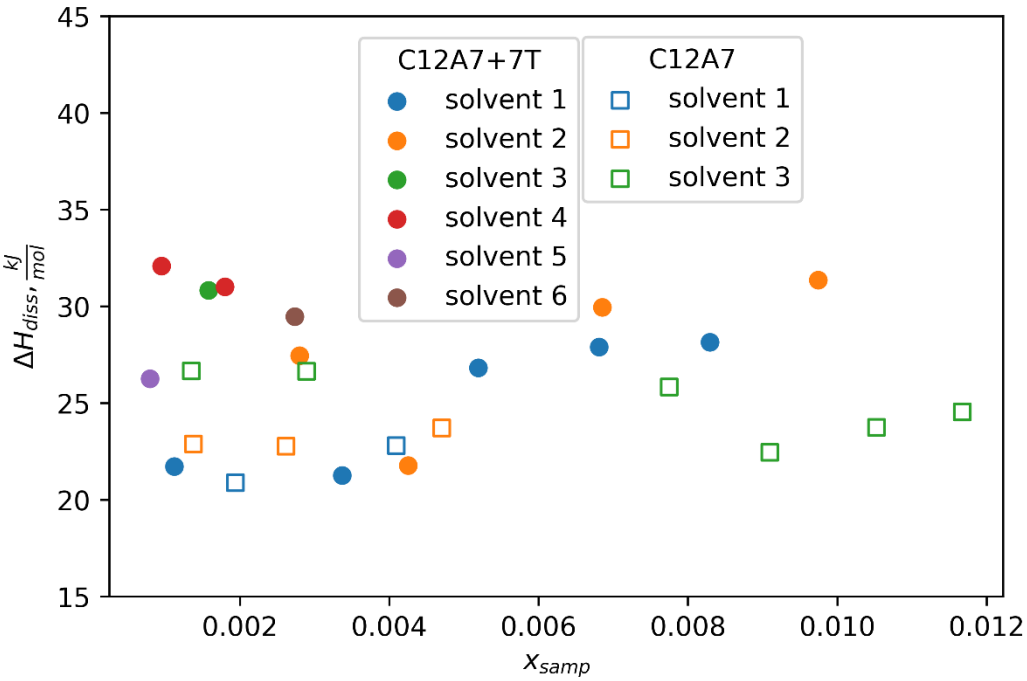

a)

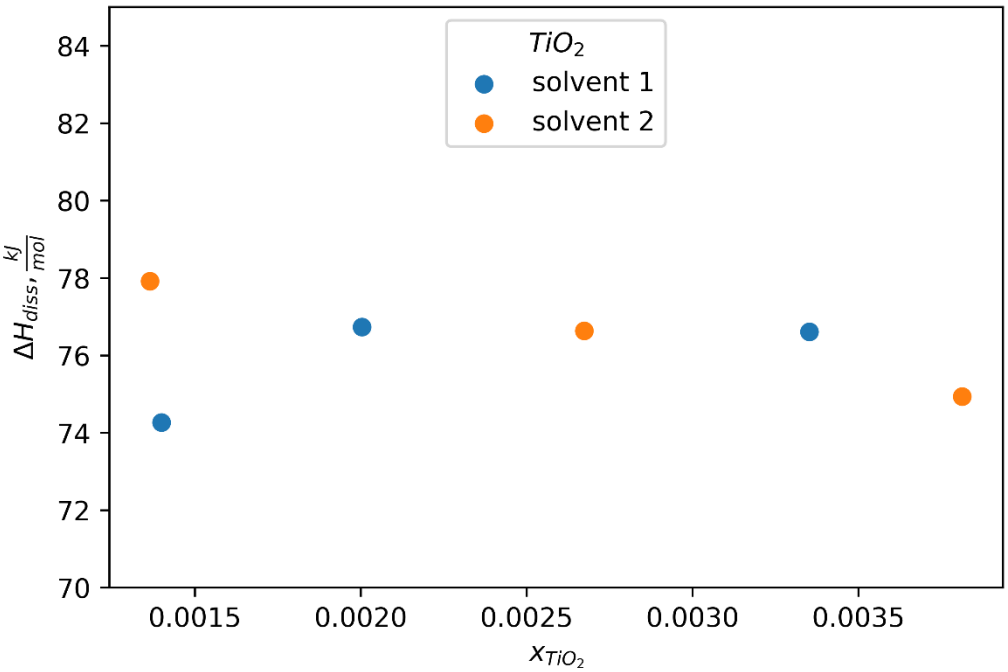

b)

Figure 3. The dependence of the enthalpy of dissolution vs mole fraction of the dissolve sample in the lead borate solvent at 1073.15 K a) of C12A7 and C12A7+7T samples (m_{solv}=30.00±0.05 g), b) of TiO_2 (rutile) (m_{solv}=20.00±0.05 g).

In addition, drop solution experiments of TiO_2 (rutile) in lead borate solvent at 1073.15 K were conducted. All raw data of these experiments are also summarized and listed in Table S4 in the Supplementary Information. The dependence of the enthalpy of dissolution of TiO_2 as mole fraction of the dissolved sample in the lead borate solvent was calculated and plotted in Figure 3b. Again, no composition dependence of the thermal effect on the total amount of TiO_2 in the lead borate solvent was revealed.

The thermochemical cycles for calculating the enthalpy of formation from oxides of C12A7 and C12A7+7T samples are listed in Tables 7, 8. In addition, the averaging values of enthalpy of dissolution in lead borate solvent at 1073.15 K of C12A7, C12A7+7T and TiO_2 samples, literature data for CaO [27] and Al_2O_3 [28] are also presented in these Tables. It should be noticed that one drop of C12A7 sample (line 8 from Table S4) was removed from the calculations because of relatively excess mass of the sample (20.81 mg) to avoid the appearance of the systematic errors in the resulting enthalpies because of different pickup of heat during fall into the hot zone of the calorimeter.

Table 7. Thermochemical cycle for calculation of the enthalpy of formation from oxides of C12A7 glass sample from drop solution calorimetry. Number of drops are presented in brackets.

$CaO_{(cr, 298.15)} \rightarrow CaO_{(diss, 1073.15)}$	ΔH_1 = -7.08±2.31 kJ/mol [27]
$\alpha\text{-}Al_2O_{3(cr, 298.15)} \rightarrow Al_2O_{3(diss, 1073.15)}$	ΔH_2 = 120.12±0.17 kJ/mol [28]
$(CaO)_{0.632}(Al_2O_3)_{0.368(gl, 298.15)} \rightarrow (CaO)_{0.632}(Al_2O_3)_{0.368(diss, 1073.15)}$	ΔH_3 = 23.7±1.1 kJ/mol [this work] (10)
$0.632CaO_{(cr, 298.15)} + 0.368Al_2O_{3(cr, 298.15)} \rightarrow (CaO)_{0.632}(Al_2O_3)_{0.368(gl, 298.15)}$	$\Delta_f H_{ox,298.15}(C12A7, gl)$
$\Delta_f H_{ox,298.15}(C12A7, gl) = 0.632\Delta H_1 + 0.368\Delta H_2 - \Delta H_3 = 16.0 \pm 1.8$ kJ/mol	

Table 8. Thermochemical cycle for calculation of the enthalpy of formation from oxides of C12A7+7T glass sample from drop solution calorimetry. Number of drops are presented in brackets.

$CaO_{(cr,\ 298.15)} \rightarrow CaO_{(diss,\ 1073.15)}$	ΔH_1 = -7.08±2.31 kJ/mol [27]
$\alpha\text{-}Al_2O_{3\ (cr,\ 298.15)} \rightarrow Al_2O_{3\ (diss,\ 1073.15)}$	ΔH_2 = 120.12±0.17 kJ/mol [28]
$TiO_2\ (rut)_{(cr,\ 298.15)} \rightarrow TiO_{2\ (diss,\ 1073.15)}$	ΔH_3 = 76.2±1.1 kJ/mol [this work] (6)
$(CaO)_{0.591}(Al_2O_3)_{0.345}(TiO_2)_{0.064\ (gl,\ 298.15)} \rightarrow (CaO)_{0.591}(Al_2O_3)_{0.345}(TiO_2)_{0.064\ (diss,\ 1073.15)}$	ΔH_4 = 27.6±2.0 kJ/mol [this work] (14)
$0.591CaO_{(cr,\ 298.15)} + 0.345Al_2O_{3\ (cr,\ 298.15)} + 0.064TiO_{2\ (cr,\ 298.15)} \rightarrow (CaO)_{0.591}(Al_2O_3)_{0.345}(TiO_2)_{0.064\ (gl,\ 298.15)}$	$\Delta_f H_{ox,298.15}(C12A7 + 7T, gl)$
$\Delta_f H_{ox,298.15}(C12A7 + 7T, gl) = 0.591\Delta H_1 + 0.345\Delta H_2 + 0.064\Delta H_3 - \Delta H_4 = 14.5 \pm 2.4$ kJ/mol	

3.3.High temperature drop calorimetry

The measured heat effect of the transposed temperature drop calorimetry measurements of C12A7 sample is summed up in Table 9. For the two measurement temperatures 998 °C / 1271.15 K and 1098 °C / 1371.15 K – the first drop corresponds to the enthalpy of crystallization at selected T ($H^{o}_{cr}(T)$ – $H^{o}_{gl}(298.15)$) and the second drop to the heat content of the crystalline compound ($H^{o}_{cr}(T)$ – $H^{o}_{cr}(298.15)$). Powder XRD measurements (see Figure S2) after the second drop revealed that all samples correspond to pure crystalline $Ca_{12}Al_{14}O_{33}$ (mayenite). The enthalpy of crystallization of C12A7 glass at 298.15 K ($H^{o}_{gl}(298.15)$ – $H^{o}_{cr}(298.15)$) was found from the two drops and corresponding values are presented in Table 9.

Table 9. The measured enthalpy of the transposed temperature drop calorimetry measurements of C12A7 sample and the calculated enthalpy of crystallization of C12A7 glass at 298.15 K.

T, K	$H^{o}_{cr}(T) - H^{o}_{gl}(298.15)$, $\frac{kJ}{mol}$	$H^{o}_{cr}(T) - H^{o}_{cr}(298.15)$, $\frac{kJ}{mol}$	$H^{o}_{gl}(298.15) - H^{o}_{cr}(298.15)$, $\frac{kJ}{mol}$
1271	57.6±1.6	72.0±1.4	14.4±2.1
1371	65.4±1.7	79.4±1.4	14.0±2.2

A mean value was calculated from the two individual measurements and a value of 14.2±2.2 kJ/mol was obtained for the crystallization reaction of C12A7 glass at 298.15 K.

The following thermochemical cycle (see Table 10) was used for the calculation of the enthalpy of formation from oxides of C12A7 glass sample. The two different values were found in the literature for the enthalpy of formation from oxides for crystalline C12A7: -2.3±0.5 kJ/mol [35] and -4.18±0.59 kJ/mol [36]. However, Trofymluk et al [35] conducted the high-temperature drop solution experiments for the series of $Ca_{12}Al_{14}O_{33\pm\delta}$ samples and noted that the value -4.2±0.2 kJ/mol for $Ca_{12}Al_{14}O_{33.46}$ sample are close with -4.18±0.59 kJ/mol obtained by enthalpy of solution measurement by Coughlin et al [36]. Thus, it was concluded that Coughlin et al [36] did not use a stoichiometric C12A7 sample in their measurement. In this case, the value -2.3±0.5 kJ/mol [35] was used for the further calculations in this work.

Table 10. Thermochemical cycle for calculation of the enthalpy of formation from oxides of C12A7 glass sample from transposed temperature drop calorimetry.

$0.632CaO_{(cr,\ 298.15)} + 0.368Al_2O_{3\ (cr,\ 298.15)} \rightarrow (CaO)_{0.632}(Al_2O_3)_{0.368\ (cr,\ 298.15)}$	ΔH_1 = -2.3±0.5 kJ/mol [35]
$(CaO)_{0.632}(Al_2O_3)_{0.368\ (cr,\ 298.15)} \rightarrow (CaO)_{0.632}(Al_2O_3)_{0.368\ (gl,\ 298.15)}$	ΔH_2 = 14.2±2.2 kJ/mol [this work]
$0.632CaO_{(cr,\ 298.15)} + 0.368Al_2O_{3\ (cr,\ 298.15)} \rightarrow (CaO)_{0.632}(Al_2O_3)_{0.368\ (gl,\ 298.15)}$	$\Delta_f H_{ox,298.15}(C12A7, gl)$
$\Delta_f H_{ox,298.15}(C12A7, gl) = \Delta H_1 + \Delta H_2 = 11.9 \pm 2.3$ kJ/mol	

4. Discussion

4.1.Heat capacity of C12A7 glass and Boson peak

In the literature on thermodynamic properties in the binary CaO-Al_2O_3 system, an experimental investigation of the low-temperature heat capacity of C3A ($Ca_3Al_2O_6$) glass was found [8]. A comparison between the heat capacity of C3A [8] and C12A7 (Table S1) is presented in Figure 4. As we can see at low-temperatures the heat capacity is similar. However, when increasing the temperature, the difference between C3A and C12A7 becomes more obvious. This is due to an increase in the contribution of Al_2O_3 to the heat capacity of the glasses with increasing temperature.

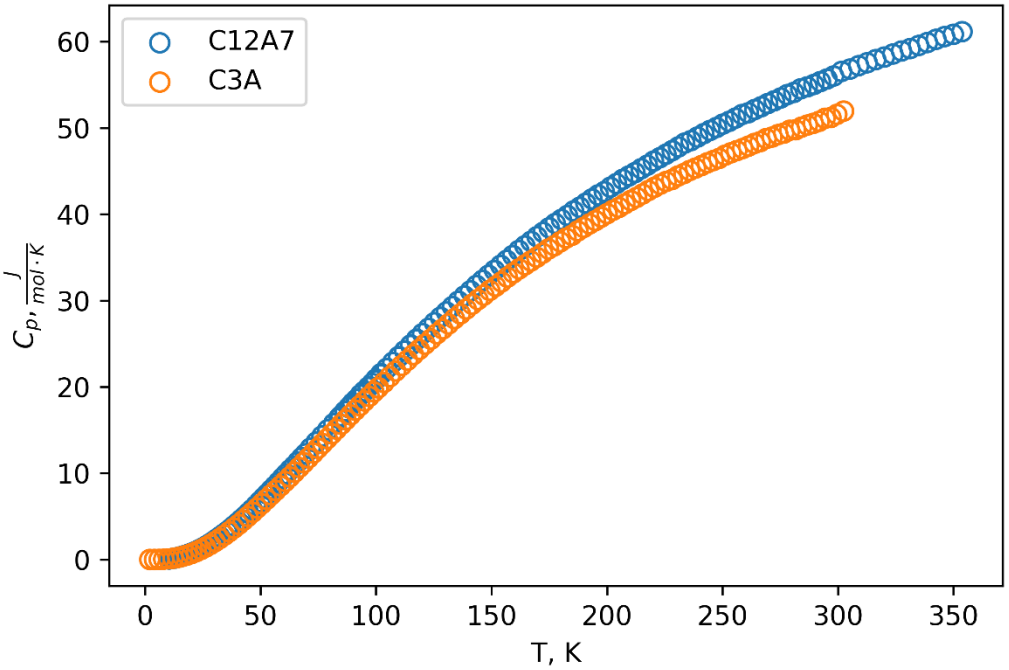

Figure 4. Heat capacities (J/(mol·K)) of C12A7 (from Table S1) and C3A (from [8]) glass samples. Data are normalized to 1 mole of formula unit of glass.

Looking from the other side at very low-temperature heat capacity we will note that in the C_p/T^3 vs T with respect to Debye T^3 law the calorimetric boson peak (maximum is roughly 18 K) is observed (Figure 5). The possible reason why this peak exists is the influence of the thermal history on C_p at very low temperatures. As it was shown in reference [37] at 10 K, for instance, the heat capacity is 50% higher for quenched than for annealed $CaMgSi_2O_6$ glass.

However, we got approximately the same behavior for our C12A7 sample and for the literature data for C3A sample [8] that was because we used the same glass synthesis procedure with similar cooling rates. The same behavior was also found for glasses in the related CaO-Al_2O_3-SiO_2 system [8,38].

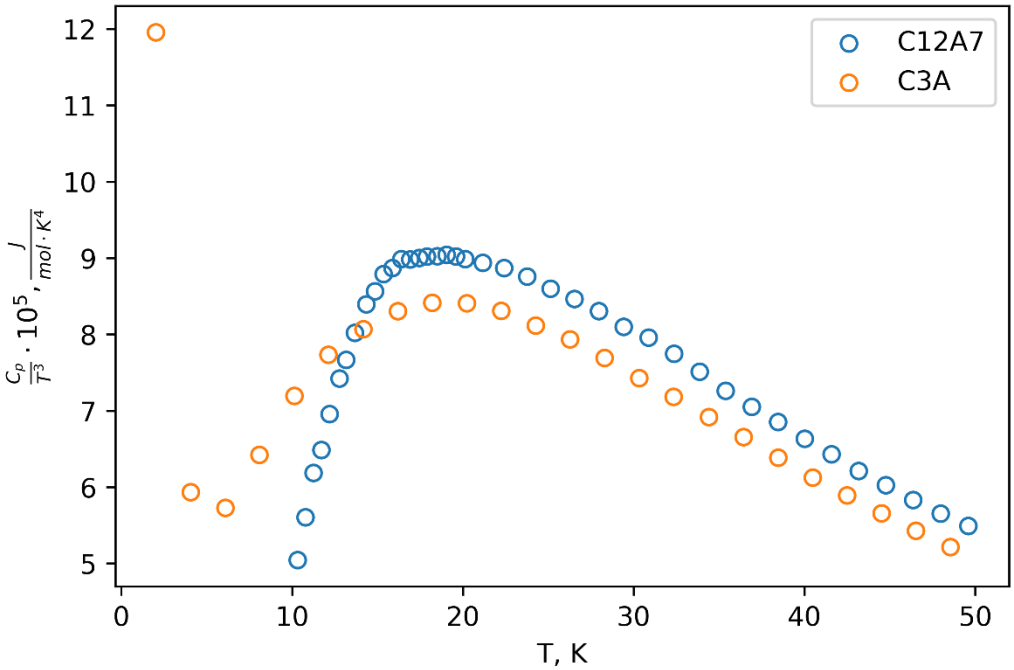

Figure 5. Deviations of the heat capacity of glasses from Debye's T^3 law. Data for C3A [8] and for C12A7 (Table S1) glass materials. Data are normalized to 1 mole of formula unit of glass.

In addition, in the same article [8] a procedure how to estimate the heat capacity of glasses in the CaO-Al_2O_3-SiO_2 system is described. The method is based on an increment-scheme of the contribution of partial molar heat capacities of pure amorphous oxides. The comparison results between the estimated heat capacity using this method and our data by the Planck-Einstein approximation of the experimental heat capacity (see Table 4) for C12A7 glass are presented in Table 11.

Table 11. Comparison C_p data of C12A7 glass between Planck-Einstein approximation of experimental data (Table 4) and estimated data using the literature [8].

T, K	C_p^{approx}	C_p^{estim}	ε, %	T, K	C_p^{approx}	C_p^{estim}	ε, %

	$\frac{J}{mol \cdot K}$				$\frac{J}{mol \cdot K}$		
50	6.789	6.608	2.7	200	42.91	42.96	-0.1
100	20.87	21.08	-1.0	250	50.38	48.84	3.1
150	33.23	33.38	-0.5	300	56.24	56.16	0.1

When analyzing the calculated data, we can say that they are rather estimates for the heat capacity of glasses. The observed deviations are random but of higher magnitude than the experimental uncertainty. Thus, it is reasonably to use them to estimate heat capacity values, but the availability of such estimates does not exclude experimental studies, which are characterized by a higher accuracy. The experimental investigation of thermodynamic properties of glasses is still required.

4.2.Enthalpy of dissolution of TiO_2 in lead borate solvent at 1073.15 K

Enthalpy of dissolution of TiO_2 (rut) in lead borate solvent at 1073.15 K was experimentally measured by drop solution calorimetry. To be sure that obtained value (76.2±1.1 kJ/mol) is suitable for the further calculations, we estimated the same value based on the literature data of $CaTiO_3$ [32]. The thermochemical cycle is presented in Table 12.

Table 12. Thermochemical cycle for calculation of the enthalpy of dissolution of TiO_2 (rut) in lead borate solvent at 1073.15 K.

$CaO_{(cr,\ 298.15)} \rightarrow CaO_{(diss,\ 1073.15)}$	ΔH_1 = -7.08±2.31 kJ/mol [27]
$CaTiO_{3\ (cr,\ 298.15)} \rightarrow CaTiO_{3\ (diss,\ 1073.15)}$	ΔH_2 = 150.86±2.90 kJ/mol [32]
$Ca_{(cr,\ 298.15)} + ½\ O_{2\ (g,\ 298.15)} \rightarrow CaO_{(cr,\ 298.15)}$	ΔH_3 = -635.09±0.88 kJ/mol [33]
$Ti_{(cr,\ 298.15)} + O_{2\ (g,\ 298.15)} \rightarrow TiO_{2\ (cr,\ 298.15)}$	ΔH_4 = -944.75±1.26 kJ/mol [33]
$Ca_{(cr,\ 298.15)} + Ti_{(cr,\ 298.15)} + {}^3/_2\ O_{2\ (g,\ 298.15)} \rightarrow CaTiO_{3\ (cr,\ 298.15)}$	ΔH_5 = -1660.6±1.7 kJ/mol [33]
TiO_2 (rut) $_{(cr,\ 298.15)} \rightarrow TiO_{2\ (diss,\ 1073.15)}$	$\Delta_{diss}H_{1073.15}(TiO_2)$
$\Delta_{diss}H_{1073.15}(TiO_2) = -\Delta H_1 + \Delta H_2 - \Delta H_3 - \Delta H_4 + \Delta H_5 = 77.2 \pm 4.4$ kJ/mol	

The enthalpy of dissolution of TiO_2 (rut) in lead borate at 1073.15 K using literature data was found as 77.2±4.4 kJ/mol. This result is in excellent agreement with our experimental value of 76.2±1.1 kJ/mol. This shows that the experimentally obtained value of the enthalpy of dissolution of TiO_2 (rut) in lead borate at 1073.15 K is thermodynamically consistent with other literature data.

4.3.Comparison of crystalline and glassy C12A7 properties

4.3.1. The heat capacity

King et al [39] published data for the low-temperature heat capacity (from 50 to 300 K) for the crystalline analogue of C12A7 sample (mineral mayenite) obtained by the adiabatic calorimetry method. The absolute difference (in J/(mol·K)) of the heat capacity for crystalline and glassy C12A7 sample ($C_{p,\mathrm{cr}} - C_{p,\mathrm{gl}}$) is presented in Figure 6. The graph was plotted as a difference between literature data for the crystalline C12A7 sample and calculated data from Equation 1 and parameters from Table 3 for the glassy C12A7 sample. As can be seen from the presented data, the heat capacity of glass is lower than the heat capacity of the crystalline phase. The relative deviation is less than 4.2%, but this difference is statistically significant keeping in mind 0.2% uncertainty for C_p according literature data and 0.4% for approximation present data by Planck-Einstein approach. This is not a typical behavior, nevertheless a similar dependence was observed for the $CaAl_2Si_2O_8$ sample [38], that is related to our C12A7 sample. From the other point of view, King [39] used the same C12A7 glass sample as Coughlin [36] for his heat of solution measurements. In this case, if the real composition of C12A7 sample in these experiments was $Ca_{12}Al_{14}O_{33.46}$ (see *3.3. High temperature drop calorimetry* in Results part), the real data for crystalline C12A7 may be shifted.

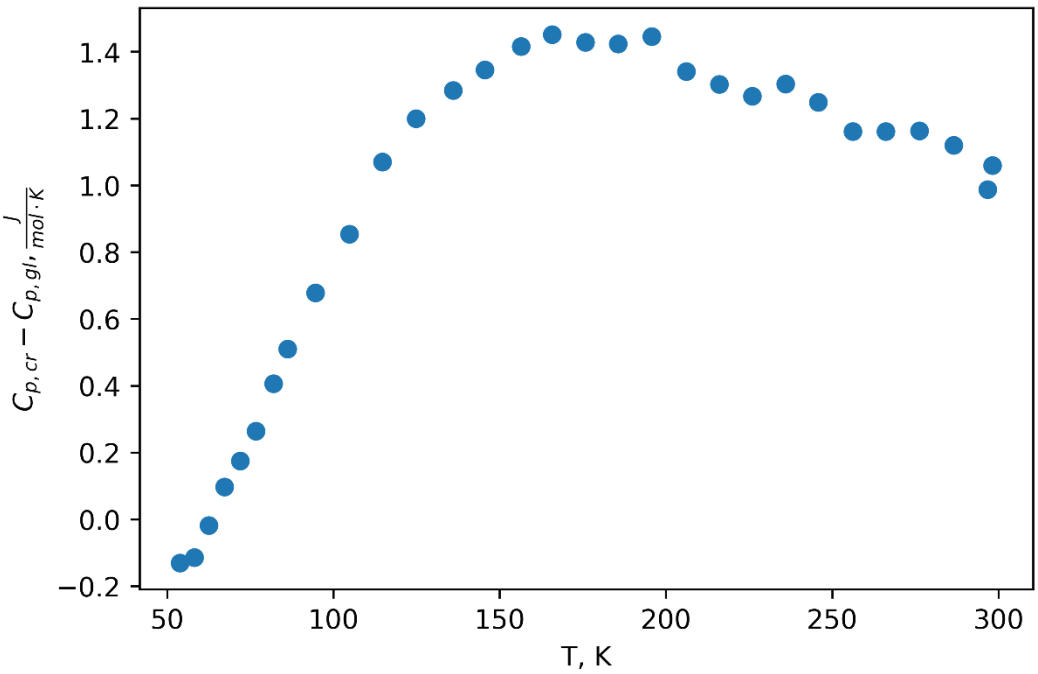

Figure 6. The absolute difference of the heat capacity for crystalline [39] and glassy (approximated by Planck-Einstein approach using Equation 1 and Table 3) C12A7 sample ($C_{p,\mathrm{cr}} - C_{p,\mathrm{gl}}$). Data are normalized to 1 mole of formula unit of glass.

4.3.2. The enthalpy of formation

Two independent experimental methods were used in this work to calculate the enthalpy of formation from oxides of C12A7 glass sample at 298.15 K ($\Delta_f H_{\mathrm{ox},298.15}(\mathrm{C12A7, gl})$): drop solution calorimetry and transposed temperature drop calorimetry. The obtained results are 16.0±1.8 kJ/mol and 11.9±2.3 kJ/mol, respectively. The values are distinguished, however, considering the uncertainties of experiments, the error bars overlap. One explanation for the underestimated values of transposed temperature drop calorimetry results may be that the studied samples were not fully crystallized after the first drop by this method. Despite the fact that after the second drop the "perfect" baseline of the powder XRD was obtained (see Figure S2), it is not confirmation of pure crystalline phase both after the first and the second drops, because of the difficulties connected with the method. However, "perfect" baseline corresponds to a very high quantity of a crystalline phase. Thus, considering that the resulting enthalpy of

formation from oxides of C12A7 glass at 298.15 K agrees within the measurement uncertainty by two independent methods we can conclude that the obtained data are reliable.

Comparing the enthalpy of formation from oxides of crystalline (-2.3±0.5 kJ/mol [35]) and glassy C12A7 sample at 298.15 K, it can be noted that they have different signs: negative for crystalline and positive for glassy. This result is completely consistent with the general ideas about the amorphous state of matter.

4.4.CAT: effect of TiO_2 addition to C12A7 on thermodynamic properties

In order to determine the impact of TiO_2 additions on thermodynamic properties of glasses in the C12A7-TiO_2 section, C12A7+5T and C12A7+7T samples were investigated by adiabatic and drop solution calorimetry.

4.4.1. Heat capacity

The results for the heat capacity of all studied samples are presented in Figure 1. The relative deviation of heat capacity C_p between the experimental data for the C12A7+5T (Table S2) and the C12A7+7T (Table S3) samples with approximation data by Planck-Einstein approach using Equation 1 and Table 3 for C12A7 sample is presented in Figure 7. As we can see, in the medium temperature range (from 75 to 350 K) the deviations for both cases are random and less than 2 standard deviations (0.2% – uncertainty of experimental data for C12A7+5T and C12A7+7T and 0.4% – uncertainty of C_p approximation of C12A7 sample using Equation 1 and parameters from Table 3), which indicates that there is no impact of TiO_2 addition on heat capacity of C12A7 up to 7 wt.% of TiO_2.

At low temperatures the discrepancies are more noticeable but, in this case, the real uncertainty of the heat capacity measurements is higher. Taking this into account, the values of the standard entropies at 298.15 K, rather than heat capacities, were compared to evaluate the influence of titanium on the thermodynamic properties of C12A7 glasses. As can be seen from Tables 4–6, all values $S^o(298.15)–S^o(0)$ are the same within the uncertainties of the determination (the difference does not exceed 0.15%). Thus, we can conclude that the entropy

of the glass at fixed temperature remains constant at the addition of titanium to C12A7 for less than 7 wt.%.

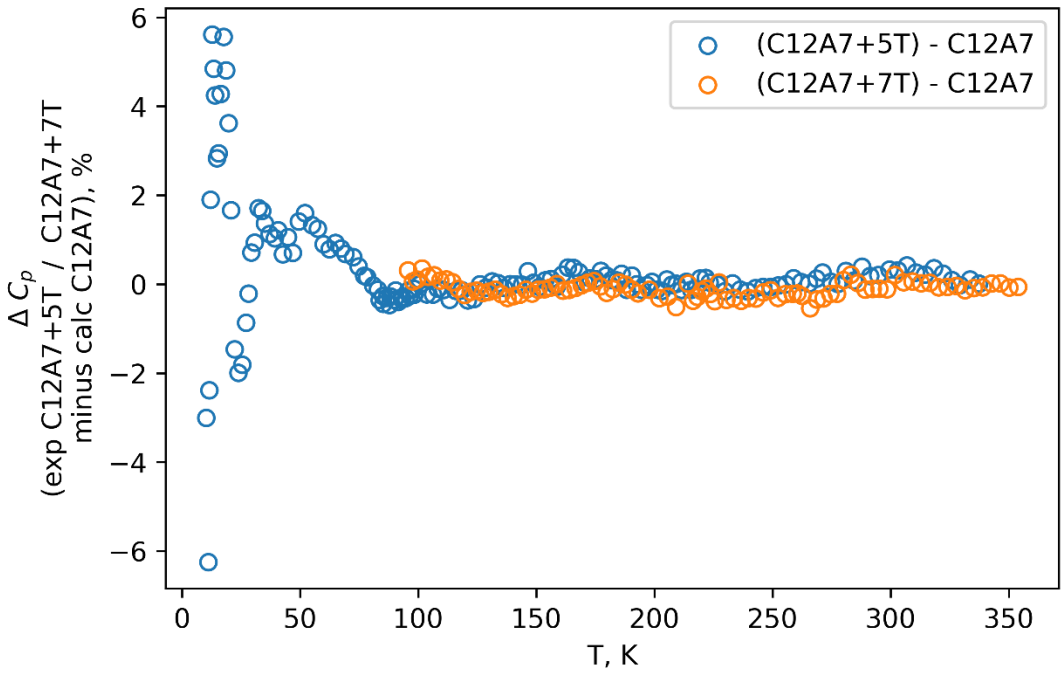

Figure 7. The relative deviation of heat capacity C_p between experimental data for C12A7+5T (Table S2) / C12A7+7T (Table S3) samples and approximation data by Planck-Einstein approach using Equation 1 and Table 3 for C12A7 sample.

4.4.2. Enthalpy of formation

If the difference of the standard entropy at 298.15 K of doped and undoped C12A7 does not exceed 0.15% (this is notably less than the uncertainty of determination), the situation for the enthalpy of formation from the pure oxides is a bit more pronounced. The values for C12A7 and C12A7+7T ($\Delta_f H_{ox}$(298.15) = 16.0□1.8 kJ/mol and 14.5±2.4 kJ/mol, respectively) are close (for C12A7 we took data obtained by drop solution experiments as the same for C12A7+7T sample); and the error bars overlap. Since it is impossible to reduce the drop-calorimetry experimental uncertainty or increase the titanium content significantly for a more noticeable effect, we see this difference as actually existing. This gives us the right to conclude that (*a*) the value of $\Delta_f H_{ox}$(298.15) is decreasing with TiO_2 increasing; (*b*) titanium additives influence to a greater extent the enthalpy term in the Gibbs free energy and (*c*) it is possible to estimate the

enthalpy of mixing of C12A7 and TiO_2 in the amorphous state with a regular solution approximation.

The estimation of $\Delta_f H^o(TiO_2$, amorph) at 298.15 K was taken from the JANAF database [40]. The thermochemical cycle from Table 13 was used to calculate the enthalpy of formation from oxide of amorphous TiO_2 at 298.15 K.

Table 13. Thermochemical cycle for calculation of the enthalpy of formation from oxide of TiO_2 amorph at 298.15 K.

$Ti_{(cr, 298.15)} + O_{2\ (g, 298.15)} \rightarrow TiO_{2\ (gl, 298.15)}$	ΔH_1 = -894.055 kJ/mol [40]
$Ti_{(cr, 298.15)} + O_{2\ (g, 298.15)} \rightarrow TiO_{2\ (cr, 298.15)}$	ΔH_2 = -944.75±1.26 kJ/mol [33]
$TiO_{2\ (cr, 298.15)} \rightarrow TiO_{2\ (gl, 298.15)}$	$\Delta_f H_{ox,298.15}(TiO_2, gl)$
$\Delta_f H_{ox,298.15}(TiO_2, gl) = \Delta H_1 - \Delta H_2 = 50.7 \pm 1.26$ kJ/mol[a]	

[a] The uncertainty was estimated from the uncertainty reported in the literature data [33]

Considering amorphous C12A7 and TiO_2 as components of a solution, a negative deviation of the enthalpy of formation from oxides at 298.15 K from the ideal-mixing straight line connecting the two end-members was observed (see Figure 8).

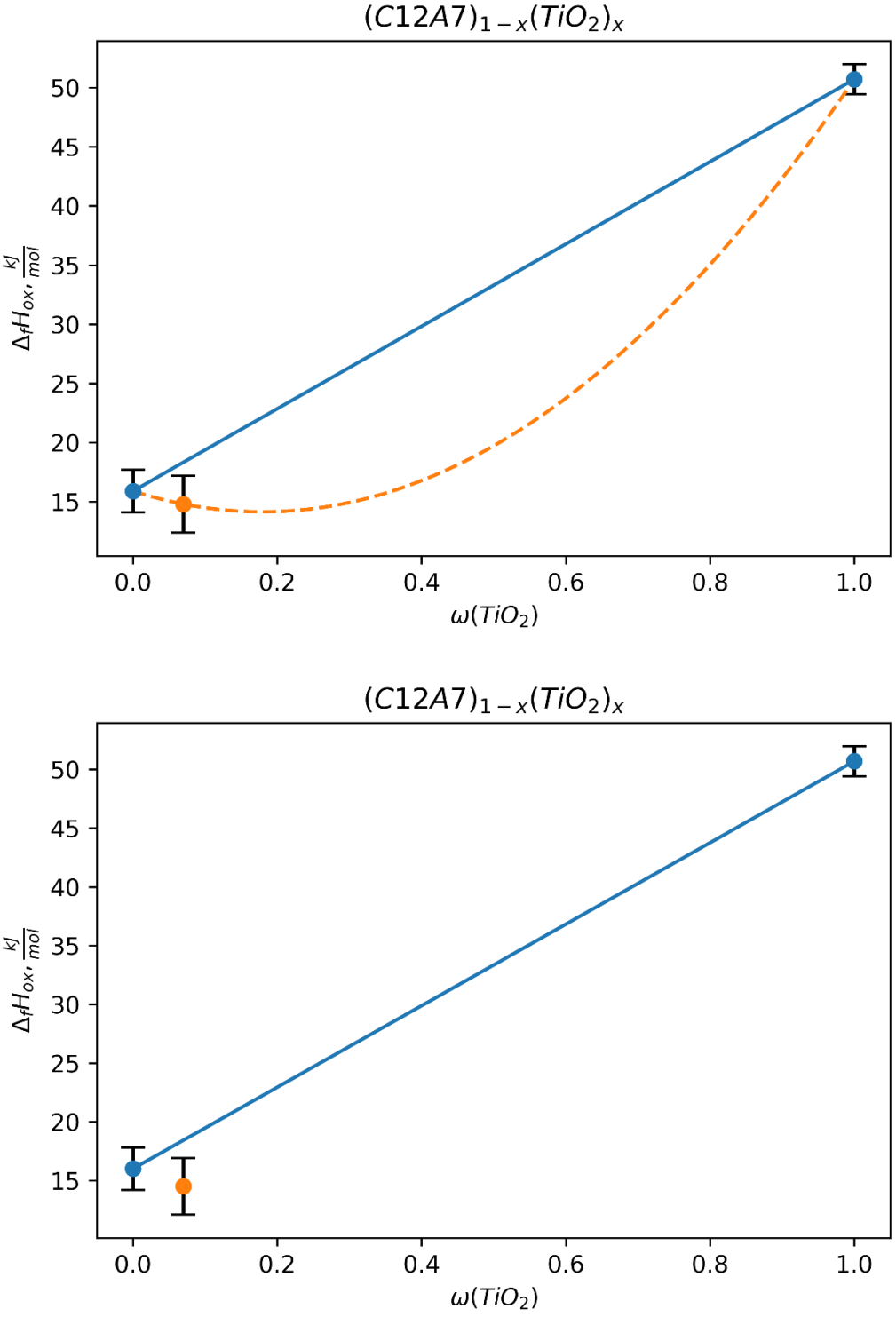

Figure 8. Enthalpy of formation from oxides of C12A7-TiO_2 solid solutions at 298.15 K. The straight line connects the two end-members. (Alex, what do think, which plot is better? The difference is only orange dashed curve. There is nowhere information about this curve. It is just for the visualization. As we understood reviewers, they did not like regular behavior and fitting

by one point. But this is not a model, just for the visualization. We can also write this to reviewers. What do you think?)

5. Conclusions

Experimental investigation of the thermodynamic properties of C12A7 binary and two C12A7+*x*TiO_2 (*x* = 5 and 7 wt.%) ternary glasses was conducted for the first time by three different calorimetric techniques: low-temperature adiabatic, high-temperature drop solution and transposed temperature drop calorimetry. The obtained heat capacity results were approximated using a semi-empirical Planck-Einstein approach. The deviations between the calculated and the experimental heat capacity for almost all points are less than 0.4% for T > 50 K, and 2% from 10 to 50 K. We believe that the parameters of the Planck-Einstein equation adequately describe the experimental data. For the high-temperature drop solution calorimetry, no composition dependence of the thermal effect on the total amount of the studied sample in the lead borate solvent at 1073.15 K were revealed. The enthalpy of formation from oxides of C12A7 and C12A7+7T glass samples was found 16.0±1.8 kJ/mol and 14.8±2.4 kJ/mol, respectively. In addition, the drop solution experiments of TiO_2 (rutile) were conducted, and the enthalpy of dissolution of TiO_2 in the lead borate solvent at 1073.15 K was found 76.2±1.1 kJ/mol, which is thermodynamically consistent with other literature data. Besides that, the independent investigation of C12A7 glass sample was performed by transposed temperature drop calorimetry at two temperatures (1271.15 and 1371.15 K). The enthalpy of formation from oxides was found 11.9±2.3 kJ/mol, that agrees within the measurement uncertainty with the result from drop solution calorimetry.

The calorimetric boson peak was observed for the C12A7 glass sample at very low temperature, which agrees with the literature data for the related samples. Comparing the estimated heat capacity of C12A7 glass from the literature and obtained experimental data, we conclude that estimated data using an additive model are a good for estimation the heat capacity of glasses, the deviations are random, but much more than experimental uncertainty. Comparing the heat capacity of crystalline and glassy C12A7 an anomaly was observed: the heat content of the crystal is higher than the one of glass.

In order to determine the impact of TiO_2 on thermodynamic properties of glasses in the C12A7-TiO_2 section, C12A7+5T and C12A7+7T samples were investigated by adiabatic and drop solution calorimetry. No impact of TiO_2 addition on the heat capacity of C12A7 up to 7 wt.% of TiO_2 was observed from 75 to 360 K. At lower temperatures there are more noticeable discrepancies, but it does not impact the entropy $S^o(T)–S^o(0)$ at higher temperatures. Thus, we can conclude that the entropy of glass at fixed temperature remains constant upon addition of titania to C12A7 for compositions less than 7 wt.% TiO_2.

The impact of TiO_2 on the enthalpy of formation from pure oxides of glasses in the C12A7-TiO_2 section is a bit more pronounced. The values for C12A7 and C12A7+7T are $\Delta_f H_{ox}(298.15)$ = 16.0□1.8 kJ/mol and 14.8±2.4 kJ/mol, respectively, and are close; the error bars overlap. But the degree of overlap is significantly less than in the case of entropy, so we can be assumed that the titanium additives impact to a greater extent the enthalpy than the entropy term in the Gibbs free energy. Thus, increasing titania additives to C12A7 glass up to 7 wt.% of TiO_2 leads to decreasing the enthalpy of formation from oxides. Considering amorphous C12A7 and TiO_2 as components of a solution, a negative deviation of the enthalpy of formation from oxides at 298.15 K from the ideal-mixing straight line connecting the two end-members was observed.

The obtained data can be used …(Alex, I think it will enough to write a couple of sentences here and in the Introduction)

CRediT authorship contribution statement

Anatoly S. Arkhipin: Investigation, Formal analysis, Writing - original draft; **Alexander Pisch**: Funding acquisition, Conceptualization, Investigation, Writing - review & editing**; Georgii M. Zhomin**: Investigation, Formal analysis, Visualization; **Semen V. Kuzovchikov**: Investigation, Writing - original draft; **Alexandra V. Khvan**: Methodology, Validation; **Natalia N. Smirnova**: Investigation, Validation; **Alexey V. Markin**: Methodology, Writing - review & editing; **Nikita A. Kovalenko**: Funding acquisition, Writing - review & editing; **Irina A. Uspenskaya**: Conceptualization, Writing - review & editing, Supervision

Declaration of Competing Interest

The authors declare that they have no known competing financial interests or personal relationships that could have appeared to influence the work reported in this paper.

Acknowledgments

The investigations were financially supported by the Russian Ministry of Science and Education, grant No. 075-15-2021-1353 and by the European Nanocem network.

Supplementary materials

Supplementary material associated with this article can be found, in the online version, at doi:

REFERENCES

[1] S. Kucharczyk, M. Zajac, C. Stabler, R.M. Thomsen, M.B. Haha, J. Skibsted, J. Deja, Structure and reactivity of synthetic CaO-Al_2O_3-SiO_2 glasses, Cem. Concr. Res. 120 (2019) 77–91. https://doi.org/10.1016/j.cemconres.2019.03.004.

[2] M. Zajac, J. Skocek, B. Lothenbach, M.B. Haha, Late hydration kinetics: Indications from thermodynamic analysis of pore solution data, Cem. Concr. Res. 129 (2020) 105975. https://doi.org/10.1016/j.cemconres.2020.105975.

[3] C.M.S. Alvares, G. Deffrennes, A. Pisch, N. Jakse, Thermodynamics and structural properties of CaO: A molecular dynamics simulation study, J. Chem. Phys. 152(8) (2020) 084503. https://doi.org/10.1063/1.5141841.

[4] N. Jakse, C.M.S. Alvares, A. Pisch, Ab initio based interionic interactions in calcium aluminotitanate oxide melts: structure and diffusion, J. Phys. Condens. Matter. 33(28) (2021) 285401. https://doi.org/10.1088/1361-648X/abfc0f.

[5] C. Téqui, R.A. Robie, B. S. Hemingway, D. R. Neuville, P. Richet, Melting and thermodynamic properties of pyrope ($Mg_3Al_2Si_3O_{12}$), Geochim. Cosmochim. Acta. 55(4) (1991) 1005–1010. https://doi.org/10.1016/0016-7037(91)90158-2.

[6] Y. Linard, I. Yamashita, T. Atake, J. Rogez, P. Richet, Thermochemistry of nuclear waste glasses: an experimental determination, J. Non. Cryst. Solids. 286(3) (2001) 200–209. https://doi.org/10.1016/S0022-3093(01)00529-4.

[7] J. Majzlan, J.A. Tangeman, E. Dachs, Heat capacity, entropy, configurational entropy, and viscosity of magnesium silicate glasses and liquids, Phys. Chem. Miner. 48(8) (2021) 28. https://doi.org/10.1007/s00269-021-01153-7.

[8] P. Richet, A. Nidaira, D.R. Neuville, T. Atake, Aluminum speciation, vibrational entropy and short-range order in calcium aluminosilicate glasses, Geochim. Cosmochim. Acta. 73(13) (2009) 3894–3904. https://doi.org/10.1016/j.gca.2009.03.041.

[9] A.M. Zahra, C.Y. Zahra, B. Piriou, DSC and Raman studies of lead borate and lead silicate glasses, J. Non. Cryst. Solids. 155(1) (1993) 45–55. https://doi.org/10.1016/0022-3093(93)90470-I.

[10] P. Richet, Y. Bottinga, L. Denielou, J.P. Petitet, C. Tequi, Thermodynamic properties of quartz, cristobalite and amorphous SiO_2: drop calorimetry measurements between 1000 and 1800 K and a review from 0 to 2000 K, Geochim. Cosmochim. Acta. 46(12) (1982) 2639–2658. https://doi.org/10.1016/0016-7037(82)90383-0.

[11] J.F. Stebbins, D.F. Weill, I.S.E. Carmichael, L.K. Moret, High temperature heat contents and heat capacities of liquids and glasses in the system $NaAlSi_3O_8$-$CaAl_2Si_2O_8$, Contrib. Mineral. Petrol. 80(3) (1982) 276–284. https://doi.org/10.1007/BF00371357.

[12] Y. Zhang, A. Navrotsky, Thermochemistry of rare-earth aluminate and aluminosilicate glasses, J. Non. Cryst. Solids. 341(1-3) (2004) 141–151. https://doi.org/10.1016/j.jnoncrysol.2004.04.027.

[13] A. Navrotsky, Progress and new directions in high temperature calorimetry, Phys. Chem. Miner. 2(1-2) (1977) 89–104. https://doi.org/10.1007/BF00307526.

[14] A. Navrotsky, G. Peraudeau, P. McMillan, J.P. Coutures, A thermochemical study of glasses and crystals along the joins silica-calcium aluminate and silica-sodium aluminate, Geochim. Cosmochim. Acta. 46(11) (1982) 2039–2047. https://doi.org/10.1016/0016-7037(82)90183-1.

[15] P. McMillan, B. Piriou, Raman spectroscopy of calcium aluminate glasses and crystals, J. Non. Cryst. Solids. 55(2) (1983) 221–242. https://doi.org/10.1016/0022-3093(83)90672-5.

[16] D.R. Neuville, L. Cormier, A.M. Flank, V. Briois, D. Massiot, Al speciation and Ca environment in calcium aluminosilicate glasses and crystals by Al and Ca K-edge X-ray absorption spectroscopy, Chem. Geol. 213(1-3) (2004) 153–163. https://doi.org/10.1016/j.chemgeo.2004.08.039.

[17] D.R. Neuville, L. Cormier, D. de Ligny, J. Roux, A.-M. Flank, P. Lagarde, Environments around Al, Si, and Ca in aluminate and aluminosilicate melts by X-ray absorption

spectroscopy at high temperature, Am. Mineral. 93(1) (2008) 228–234. https://doi.org/10.2138/am.2008.2646.

[18] D.R. Neuville, G.S. Henderson, L. Cormier, D. Massiot, The structure of crystals, glasses, and melts along the CaO-Al_2O_3 join: Results from Raman, Al L- and K-edge X-ray absorption, and ^{27}Al NMR spectroscopy, Am. Mineral. 95(10) (2010) 1580–1589. https://doi.org/10.2138/am.2010.3465.

[19] M. Licheron, V. Montouillout, F. Millot, D.R. Neuville, Raman and ^{27}Al NMR structure investigations of aluminate glasses: $(1-x)Al_2O_3-xMO$, with M = Ca, Sr, Ba and $0.5<x<0.75$), J. Non. Cryst. Solids. 357(15) (2011) 2796–2801. https://doi.org/10.1016/j.jnoncrysol.2011.03.001.

[20] B. Hallstedl, Assessment of the CaO-Al_2O_3 system, J. Am. Ceram. Soc. 73(1) (1990) 15–23. https://doi.org/10.1111/j.1151-2916.1990.tb05083.x.

[21] J.A. Imlach, F.P. Glasser, Phase equilibria in the system CaO-Al_2O_3-TiO_2, Trans. Br. Ceram. Soc. 67 (1968) 581–609.

[22] R.M. Varushchenko, A.I. Druzhinina, E.L. Sorkin, Low-temperature heat capacity of 1-bromoperfluorooctane, J. Chem. Thermodyn. 29(6) (1997) 623–637. https://doi.org/10.1006/jcht.1996.0173.

[23] G.F. Voronin, I.B. Kutsenok, Universal method for approximating the standard thermodynamic functions of solids, J. Chem. Eng. Data. 58(7) (2013) 2083–2094. https://doi.org/10.1021/je400316m.

[24] A.L. Voskov, I.B. Kutsenok, G.F. Voronin, CpFit program for approximation of heat capacities and enthalpies by Einstein-Planck functions sum, Calphad. 61 (2018) 50–61. https://doi.org/10.1016/j.calphad.2018.02.001.

[25] N.Yu. Kozin, A.L. Voskov, A.V. Khvan, I.A. Uspenskaya, Thermodynamic properties of synthetic zeolite – Mordenite, Thermochim. Acta. 688 (2020) 178600. https://doi.org/10.1016/j.tca.2020.178600.

[26] Standard Material 720, Synthetic Sapphire (α-Al_2O_3), National Bureau of Standards, (1982).

[27] J. Cheng, A. Navrotsky, Energetics of $La_{1-x}A_xCrO_{3-\delta}$ perovskites (A = Ca or Sr), J. Solid State Chem. 178(1) (2005) 234–244. https://doi.org/10.1016/j.jssc.2004.11.028.

[28] A. Navrotsky, Progress and new directions in calorimetry: A 2014 perspective, J. Am. Ceram. Soc. 97(11) (2014) 3349–3359. https://doi.org/10.1111/jace.13278.

[29] R.L. Putnam, A. Navrotsky, B.F. Woodfield, J. Boerio-Goates, J.L. Shapiro, Thermodynamics of formation for zirconolite ($CaZrTi_2O_7$) from T = 298.15 K to T = 1500 K, J. Chem. Thermodyn. 31(2) (1999) 229–243. https://doi.org/10.1006/jcht.1998.0445.

[30] www.factsage.com, FactSage FTPs database, 8.2.

[31] www.sgte.net, SGTE pure substance database, 11.0.

[32] J. Linton, A. Navrotsky, Y. Fei, The thermodynamics of ordered perovskites on the $CaTiO_3$-$FeTiO_3$ join, Phys. Chem. Miner. 25(8) (1998) 591–596. https://doi.org/10.1007/s002690050152.

[33] R.A. Robie, B.S. Hemingway, Thermodynamic properties of minerals and related substances at 298.15 K and 1 bar (10^5 Pascals) pressure and at higher temperatures, US Government Printing Office, 1995.

[34] O. Knacke, O. Kubaschewski, R. Hesselman, Thermochemical properties of inorganic substances, 2nd ed., Springer, Berlin, 1991.

[35] O. Trofymluk, Y. Toda, H. Hosono, A. Navrotsky, Energetics of formation and oxidation of microporous calcium aluminates: A new class of electrides and ionic conductors, Chem. Mater. 17(22) (2005) 5574–5579. https://doi.org/10.1021/cm051662w.

[36] J.P. Coughlin, Heats of formation of crystalline $CaO{\cdot}Al_2O_3$, $12CaO{\cdot}7Al_2O_3$ and $3CaO{\cdot}Al_2O_3$, J. Am. Chem. Soc. 78(21) (1956) 5479–5482.

[37] P. Richet, R.A. Robie, B.S. Hemingway, Low-temperature heat capacity of diopside glass ($CaMgSi_2O_6$): A calorimetric test of the configurational-entropy theory applied to the viscosity of liquid silicates, Geochim. Cosmochim. Acta. 50(7) (1986) 1521–1533. https://doi.org/10.1016/0016-7037(86)90326-1.

[38] P. Richet, R.A. Robie, B.S. Hemingway, Entropy and structure of silicate glasses and melts, Geochim. Cosmochim. Acta. 57(12) (1993) 2751–2766. https://doi.org/10.1016/0016-7037(93)90388-D.

[39] E.G. King, Heat capacities at low temperatures and entropies at 298.16 K of crystalline calcium and magnesium aluminates, J. Phys. Chem. 59 (1955) 218–219.

[40] M.W. Chase, NIST-JANAF thermochemical tables, 4th ed., J. Phys. Chem. Ref. Data Monogr. 9, 1998.